Inorganic Chemistry

Article

pubs.acs.org/IC

New Tetracopper(II) Cubane Cores Driven by a Diamino Alcohol: Self-assembly Synthesis, Structural and Topological Features, and Magnetic and Catalytic Oxidation Properties

Sara S. P. Dias,[†] Marina V. Kirillova,[†] Vânia André,[†] Julia Kłak,[‡] and Alexander M. Kirillov*[,†]

[†]Centro de Química Estrutural, Complexo I, Instituto Superior Técnico, Universidade de Lisboa, Avenida Rovisco Pais, 1049-001 Lisbon, Portugal

[‡]Faculty of Chemistry, University of Wrocław, ul. F. Joliot-Curie 14, 50-383 Wroclaw, Poland

Supporting Information

ABSTRACT: Two new coordination compounds with tetracopper(II) cores, namely, a 1D coordination polymer, $[Cu_4(\mu_4\text{-}H_2edte)(\mu_5\text{-}H_2edte)(sal)_2]_n \cdot 10nH_2O$ (**1**), and a discrete 0D tetramer, $[Cu_4(\mu_4\text{-}Hedte)_2(Hpmal)_2(H_2O)] \cdot 7.5H_2O$ (**2**), were easily self-assembled from aqueous solutions of copper(II) nitrate, *N*,*N*,*N*′,*N*′-tetrakis(2-hydroxyethyl)ethylenediamine (H_4edte), salicylic acid (H_2sal), or phenylmalonic acid (H_2pma). The obtained compounds were characterized by IR and electron paramagnetic resonance spectroscopy, thermogravimetric and elemental analysis, and single-crystal X-ray diffraction. In addition to different dimensionalities, their structures reveal distinct single-open $[Cu_4(\mu_2\text{-}O)(\mu_3\text{-}O)_3]$ (in **1**) or double-open $[Cu_4(\mu_2\text{-}O)_2(\mu_3\text{-}O)_2]$ (in **2**) cubane cores with 3M4-1 topology. In crystal structures, numerous crystallization water molecules are arranged into the intricate infinite 1D $\{(H_2O)_{18}\}_n$ water tapes (in **1**) or discrete $(H_2O)_9$ clusters (in **2**) that participate in multiple hydrogen-bonding interactions with the metal−organic hosts, thus extending the overall structures into very complex 3D supramolecular networks. After simplification, their topological analysis revealed the binodal 6,10- or 6,8-connected underlying 3D nets with unique or rare 6,8T2 topology in **1** and **2**, respectively. The magnetic properties of **1** and **2** were investigated in the 1.8−300 K temperature range, indicating overall antiferromagnetic interactions between the adjacent Cu^{II} ions within the $[Cu_4O_4]$ cores. The obtained compounds also act as bioinspired precatalysts for mild homogeneous oxidation, by aqueous hydrogen peroxide at 50 °C in an acidic $MeCN/H_2O$ medium, of various cyclic and linear C_5−C_8 alkanes to the corresponding alcohols and ketones. Overall product yields of up to 21% (based on alkane) were achieved, and the effects of various reaction parameters were studied.

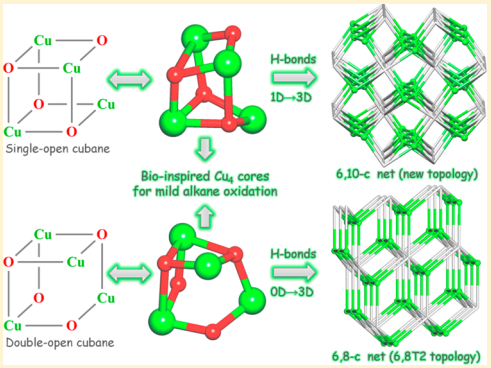

INTRODUCTION

Amino alcohols are recognized N,O building blocks for the design of coordination compounds that include a diversity of discrete multinuclear metal complexes, clusters, and molecular wheels, as well as various coordination polymers and metal−organic frameworks.[1−3] Owing to their different functional properties, these amino alcohol driven compounds have found notable applications in areas ranging from molecular magnetism and catalysis to supramolecular chemistry and crystal engineering.[3−7]

Among the variety of simple amino alcohols (e.g., *N*,*N*-dimethylethanolamine, diethanolamine, and triethanolamine), *N*,*N*,*N*′,*N*′-tetrakis(2-hydroxyethyl)ethylenediamine (H_4edte) represents an interesting multidentate diamine with four ethyl alcohol groups. However, in spite of its low cost and commercial availability, water solubility and stability, potential coordination flexibility and versatility, the application of H_4edte toward the design of multinuclear metal complexes and, in particular, coordination polymers has remained underexplored.[1,6,7] Although some notable examples of high-nuclearity Mn[6] and Fe[7] clusters driven by H_4edte have been reported, the coordination chemistry of H_4edte toward Cu is still limited to single mono- or dicopper(II) complexes,[5a,8] as attested by a search of the Cambridge Structural Database.[1]

Bearing these points in mind and following our general interest in the exploration of various amino alcohol building blocks for the generation, by a simple aqueous medium self-assembly method, of diverse functional multicopper(II) complexes and coordination polymers,[3,5] the principal objectives of the current work consisted of (i) opening up the application of H_4edte for the preparation of new discrete and polymeric multicopper(II) derivatives, (ii) identifying their structural and topological features, and (iii) studying their magnetic and catalytic behavior.

Hence, we report herein the aqueous medium self-assembly generation, full characterization, crystal structures, topological analysis, and magnetic and oxidation catalytic properties of two

Received: January 7, 2015
Published: May 14, 2015

DOI: 10.1021/acs.inorgchem.5b00048
Inorg. Chem. 2015, 54, 5204−5212

novel H_4edte-driven tetracopper(II) compounds, namely, a 1D coordination polymer, $[Cu_4(\mu_4\text{-}H_2edte)(\mu_5\text{-}H_2edte)(sal)_2]_n \cdot 10nH_2O$ (**1**), and a discrete 0D tetramer, $[Cu_4(\mu_4\text{-}Hedte)_2(Hpmal)_2(H_2O)]\cdot 7.5H_2O$ (**2**). Apart from representing the first multicopper clusters derived from H_4edte,[1] both compounds also display distinct single- or double-open $[Cu_4O_4]$ cubane cores, act as metal−organic matrixes to store intricate water clusters, reveal the formation of complex 3D supramolecular networks with undocumented or rare topologies, and function as promising bioinspired precatalysts for the mild oxidation of different cyclic and linear C_5−C_8 alkanes to produce the corresponding alcohols and ketones.

EXPERIMENTAL SECTION

General Synthetic Procedure and Characterization for 1 and 2. To an aqueous 0.1 M solution of $Cu(NO_3)_2\cdot 3H_2O$ (10 mL, 1 mmol) was added an aqueous 1 M solution of *N*,*N*,*N*′,*N*′-tetrakis(2-hydroxyethyl)ethylenediamine (H_4edte; 0.5 mL, 0.5 mmol) with continuous stirring at room temperature. Then, salicylic acid (H_2sal; 138 mg, 1 mmol) for **1** or phenylmalonic acid (H_2pmal; 90 mg, 0.5 mmol) for **2** and an aqueous 1 M solution of NaOH (3 mL, 3 mmol; up to pH ∼8) were added to the reaction mixture. The resulting solution was stirred for 1 day and then filtered off. The filtrate was left to evaporate in a beaker at room temperature. Green crystals (including those suitable for single-crystal X-ray diffraction) were formed in 1 month, then collected, and dried in air to furnish compounds **1** and **2** in ∼50% yield, based on copper(II) nitrate.

*$[Cu_4(\mu_4\text{-}H_2edte)(\mu_5\text{-}H_2edte)(sal)_2]_n\cdot 10nH_2O$ (**1**).* Anal. Calcd for **1** − $3H_2O$ ($Cu_4C_{34}H_{66}N_4O_{21}$; MW 1121.1): C, 36.43; H, 5.93; N, 5.00. Found: C, 36.11; H, 5.67; N, 4.87. IR (KBr, cm^{-1}): ν(OH) 3362 (s br), ν(CH) 2864 (s br), ν_{as}(COO) 1602 (s), 1566 (s), and 1528 (s), ν_s(COO) 1453 (s) and 1377 (s), 1320 (m), ν(C−X) (X = C, N, O) 1253 (s), 1142 (m), and 1066 (s br), 887 (m br), 834 (w), 768 (m), 712 (w), 639 (w), 585 (w), 494 (w). ESI-MS(±) (MeCN/H_2O): selected fragments with relative abundance >5%. MS(−): *m*/*z* 994 (100%) $[Cu_4(H_2edte)_2(sal)_2 - H]^-$, 949 (15%) $[Cu_4(H_2edte)_2(sal)_2 - CH_2CH_2OH]^-$. MS(+): *m*/*z* 858 (5%) $[Cu_4(Hedte)_2(Hsal)]^+$, 796 (15%) $[Cu_3(H_2edte)_2(Hsal)]^+$, 641 $[Cu_4(Hedte)(sal)(H_2O)]^+$, 597 (100%) $[Cu_4(Hedte)(sal)(H_2O) - CH_2CH_2OH]^+$.

*$[Cu_4(\mu_4\text{-}Hedte)_2(Hpmal)_2(H_2O)]\cdot 7.5H_2O$ (**2**).* Anal. Calcd for **2** ($Cu_4C_{38}H_{73}N_4O_{24.5}$, MW 1232.2): C, 37.04; H, 5.97; N, 4.55. Found: C, 37.03; H, 5.50; N, 4.54. IR (KBr): ν(OH) 3419 (s br), ν(CH) 2856 (m), ν_{as}(COO) 1624 (s br) and 1597 (s), ν_s(COO) 1409 (m) and 1395 (m), ν(C−X) (X = C, N, O) 1274 (w), 1059 (m), and 1034 (w), 906 (w), 730 (m), 637 (w), 504 (w).

X-ray Crystallography. Crystals of **1** and **2** suitable for X-ray diffraction study were mounted with Fomblin in a cryoloop. Data were collected on a Bruker AXS-Kappa APEX II diffractometer with graphite-monochromated radiation (Mo Kα, λ = 0.17073 Å). The X-ray generator was operated at 50 kV and 30 mA, and the X-ray data collection was monitored by the *APEX2* program.[9] All data were corrected for Lorentzian, polarization, and absorption effects with the *SAINT* and *SADABS* programs.[9] *SIR97*[10] and *SHELXS-97*[11] were used for structure solution, and *SHELXL-97*[11] was applied for full-matrix least-squares refinement on F^2. These three programs are included in the package of programs *WINGX*, version 1.80.05.[12] Non-H atoms were refined anisotropically. A full-matrix least-squares refinement was used for the non-H atoms with anisotropic thermal parameters. All of the H atoms were inserted in idealized positions and allowed to refine in the parent C or O atom, except for the hydroxide H atoms in the amino alcohol ligands, which were located from the electron density map. It was not possible to locate the water H atoms. In both structures, there are disordered water molecules (O9w, O10w, O11w, and O12w in compound **1** and O8w in compound **2**) with 0.5 occupancy factors; in the specific case of compound **2**, O8w resides near special positions, and thus both positions are nearby. *TOPOS 4.0*[13] and *PLATON*[14] were used for topological analysis and hydrogen-bonding interactions, respectively. Crystal data and details of data collection for **1** and **2** are reported in Table 1.

Table 1. Crystal Data and Structure Refinement Details for Compounds 1 and 2

	1	**2**
formula	$Cu_4C_{34}H_{52}N_4O_{23}$	$Cu_4C_{38}H_{56}N_4O_{23.5}$
fw	1139	1199
cryst form, color	plate, green	plate, blue
cryst size (mm)	0.2 × 0.1 × 0.02	0.2 × 0.15 × 0.04
cryst syst	orthorhombic	triclinic
space group	*Pbca*	$P\bar{1}$
a, Å	17.7705(9)	12.838(6)
b, Å	22.3871(12)	13.677(4)
c, Å	23.5210(13)	15.199(3)
α, deg	90	85.959(5)
β, deg	90	83.915(6)
γ, deg	90	69.114(4)
Z	8	2
V, Å	9357.4(9)	2477.8(15)
T, K	150(2)	293(2)
D_c, g cm^{-3}	1.617	1.607
μ(Mo Kα), mm^{-1}	1.878	1.779
θ range (deg)	2.27−26.37	2.26−26.35
reflns collected	63901	42251
indep reflns	9487	10015
R_{int}	0.1308	0.0669
R1,[a] wR2[b] [$I \geq 2\sigma(I)$]	0.0943, 0.1671	0.0558, 0.1511
GOF on F^2	1.105	1.010

[a] $R1 = \sum||F_o| - |F_c||/\sum|F_o|$. [b] $wR2 = [\sum[w(F_o^2 - F_c^2)^2]/\sum[w(F_o^2)^2]]^{1/2}$.

Magnetic Studies. The magnetization of powdered samples **1** and **2** was measured over the 1.8−300 K temperature range using a Quantum Design SQUID-based MPMSXL-5-type magnetometer. The superconducting magnet was generally operated at a field strength ranging from 0 to 5 T. Sample measurements were made at a magnetic field of 0.5 T. The SQUID magnetometer was calibrated with the palladium rod sample. Corrections are based on subtraction of the sample-holder signal, and the χ_D contribution was estimated from Pascal's constants.[15]

Catalytic Studies. The alkane oxidations were carried out in an air atmosphere in thermostated Pyrex reactors equipped with a condenser, under vigorous stirring at 50 °C, and using acetonitrile (MeCN) as the solvent (up to 5.0 mL total volume). In a typical experiment, a solid precatalyst, **1** or **2** (0.01 mmol), and gas chromatography (GC) internal standard ($MeNO_2$, 50 μL) were introduced into a MeCN solution, followed by the addition of an acid promoter (0.01−0.20 mmol) used as a stock solution in MeCN. The alkane substrate (2 mmol) was then introduced, and the reaction started upon the addition of hydrogen peroxide (H_2O_2; 50% in water, 10 mmol) in one portion. The reactions were monitored by withdrawing small aliquots after different periods of time, which were treated with PPh_3 (following a method developed by Shul'pin)[16] for reduction of the remaining H_2O_2 and alkyl hydroperoxides that are typically formed as major primary products in alkane oxidation. The samples were analyzed by GC using nitromethane as an internal standard. Attribution of the peaks was made by a comparison with the chromatograms of authentic samples. Chromatographic analyses were run on an Agilent Technologies 7820A series gas chromatograph (helium as the carrier gas) equipped with a flame ionization detector and a BP20/SGE (30 m × 0.22 mm × 0.25 μm) capillary column. Blank tests confirmed that alkane oxidation does not proceed in the absence of a copper precatalyst. Given a possibility of alkane oxidation by Cu ions in the presence of trifluoroacetic acid (TFA),[17] control tests were also performed for the oxidation of cyclohexane by H_2O_2

DOI: 10.1021/acs.inorgchem.5b00048
Inorg. Chem. 2015, 54, 5204−5212

with copper(II) nitrate as a precatalyst (reaction conditions were those of Table 2), either in the absence or in the presence of a TFA promoter, resulting in 3.0 or 3.1% total product yield, respectively. These yields are significantly inferior to those achieved in the **1**/TFA/H_2O_2 (13.5%) or **2**/TFA/H_2O_2 (16.2%) systems (Table 2), thus confirming the influence of ligands and their structural arrangement in the precatalysts **1** and **2** on the observed catalytic behavior.

Table 2. Mild Oxidation of Different C_5−C_8 Alkanes by the 1/TFA/H_2O_2 and 2/TFA/H_2O_2 Systems[a]

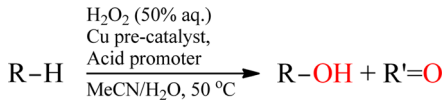

alkane (R−H)	total yield of oxidation products, %[b]	
	1/TFA/H_2O_2	**2**/TFA/H_2O_2
cyclopentane	7.2	8.9
cyclohexane	13.5	16.2
cycloheptane	21.2	19.8
cyclooctane	16.0	19.3
n-pentane	3.1	2.8
n-hexane	4.2	6.1
n-heptane	10.2	9.4
n-octane	4.4	4.5

[a]Reaction conditions: precatalyst **1** or **2** (0.01 mmol), TFA (0.05 mmol), alkane (1.0 mmol), H_2O_2 (50% aq, 5.0 mmol), MeCN (up to 5 mL total volume), 50 °C, 3 h. [b]Based on an alkane substrate, calculated from GC analysis after treatment of the reaction mixture with PPh_3; total yields [(moles of products per mole of substrate) × 100%] correspond to the sum of yields of cyclic alcohols and ketones in the case of cycloalkane oxidation or to the sum of yields of various isomeric alcohols and ketones (aldehydes) in the case of *n*-alkane oxidation; for yields of each product, see Table S1 in the SI.

RESULTS AND DISCUSSION

Synthesis. To probe the use of H_4edte as a multidentate amino alcohol building block for the synthesis of multicopper(II) coordination compounds, we applied an aqueous medium self-assembly method. Thus, a simple combination, in a water solution at ∼25 °C in air, of copper(II) nitrate with H_4edte as a main building block, salicylic (H_2sal) or phenylmalonic (H_2pmal) acid as an ancillary ligand (Scheme 1), and sodium hydroxide as a pH regulator resulted in the self-assembly generation of two new coordination compounds bearing tetracopper(II) cubane cores, namely, a 1D coordination polymer, $[Cu_4(\mu_4\text{-}H_2edte)(\mu_5\text{-}H_2edte)(sal)_2]_n\cdot 10nH_2O$ (**1**), and a discrete 0D tetramer, $[Cu_4(\mu_4\text{-}Hedte)_2 \times (Hpmal)_2(H_2O)]\cdot 7.5H_2O$ (**2**). The choice of H_2sal was governed by its recognized application as a simple ancillary ligand to stabilize multicopper(II) cores,[1] whereas H_2pmal was selected because of its little explored use in copper(II) coordination chemistry,[18] as well as to find out whether the presence of two aliphatic carboxylic groups in addition to a phenyl ring can affect the structure of the resulting product. However, the self-assembly of **1** and **2** appeared to be primarily guided by H_4edte as a main building block, with both ancillary acids acting as terminal ligands. The obtained products were isolated as air-stable microcrystalline materials and characterized by IR and EPR spectroscopy, thermogravimetric and elemental analysis, and single-crystal X-ray diffraction (for discussion of the spectral and thermogravimetric data, see the Supporting Information, SI).

Scheme 1. Structural Formulas of Organic Building Blocks

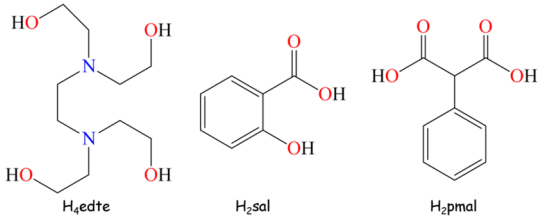

Structural and Topological Description. Compound **1** is a 1D coordination polymer, the structure of which is composed of the repeating tetracopper(II) $[Cu_4(\mu_4\text{-}H_2edte)(\mu_5\text{-}H_2edte)(sal)_2]$ units (Figure 1a) and 10 crystallization water molecules. The adjacent Cu_4 blocks reveal a single-open $[Cu_4(\mu_2\text{-}O)(\mu_3\text{-}O)_3]$ cubane core and are interconnected via one of the hydroxyethyl arms of the μ_5-H_2edte ligand, forming an infinite metal−organic chain (Figure 1b). The tetracopper(II) blocks consist of four symmetry-nonequivalent Cu atoms, two chelating salicylate(2−) ligands, one μ_4-H_2edte(2−) moiety, and one μ_5-H_2edte(2−) moiety. The five-coordinate Cu1 atom shows a distorted square-pyramidal $\{CuO_5\}$ environment (τ_5 = 0.18 in **1**; τ_5 = 0 for an idealized square-pyramidal geometry),[19a,b] filled by the salicylate O1 and O2 atoms and the amino alcohol O7 and O14 atoms [Cu1−O1 1.927(6) Å; Cu1−O2 1.890(6) Å; Cu1−O7 1.956(5) Å] in equatorial positions, whereas an axial site is taken by the $O8^i$ atom [Cu1−$O8^i$ 2.432(6) Å]. The five-coordinate Cu2 center is very similar to Cu1 in geometrical terms, with its square-pyramidal $\{CuO_5\}$ environment (τ_5 = 0.15) occupied by two sal and three H_2edte O atoms; the Cu2−O distances are in the 1.902(6)−2.404(6) Å range. The six-coordinate Cu3 atom exhibits a distorted octahedral $\{CuN_2O_4\}$ geometry, filled by the N1, N2, O9, and O13 atoms in the equatorial sites [Cu3−N1 2.099(6) Å; Cu3−N2 1.990(8) Å; Cu3−O10 1.943(6) Å; Cu3−O13 1.941(6) Å], whereas the apical positions are taken by the remaining O7 and O9 atoms of the μ_4-H_2edte moiety [Cu3−O7 2.395(5) Å; Cu3−O9 2.648(8) Å]. The six-coordinate Cu4 atom is essentially similar to Cu3, revealing even a more distorted octahedral $\{CuN_2O_4\}$ environment filled by the equatorial N3, N4, O13, and O14 atoms [Cu4−N3 2.009(8) Å; Cu4−N4 2.071(7) Å; Cu4−O13 1.901(6) Å; Cu4−O14 1.988(6) Å] and the axial O10 and O12 atoms [Cu4−O10 2.900(6) Å; Cu4−O12 2.428(8) Å] of the μ_5-H_2edte ligand, which possesses one hydroxyethyl arm connected to the Cu1 atom of an adjacent tetracopper(II) block. Although some of the Cu−O bonds [i.e., Cu3−O9 2.648(8) Å and Cu4−O10 2.900(6) Å] are rather long, these are still inferior to the sum of the van der Waals radii of the Cu and O atoms (∼2.92 Å).[19c] The four Cu centers are mutually interconnected via three μ_3-O and one μ_2-O atoms of two H_2edte moieties to generate a distorted single-open $[Cu_4(\mu_2\text{-}O)(\mu_3\text{-}O)_3]$ cubane core (Scheme 2b,e) with the Cu···Cu separations in the 3.129(2)−3.624(1) Å range (avg 3.329 Å). From the topological viewpoint,[13a,b] both regular and open $[Cu_4O_4]$ cubane cores (Scheme 2) can be classified as uninodal 3-connected motifs with 3M4-1 topology and a point symbol of (3^3). Scheme 2d shows a graph of the Cu_4 skeleton obtained after transforming the μ-O atoms in the $[Cu_4(\mu_2\text{-}O)(\mu_3\text{-}O)_3]$ core to Cu−Cu edges, by applying a method developed for the topological analysis of coordination clusters.[13a,b,19,20]

A notable feature of **1** consists of the presence of numerous crystallization water molecules that are arranged into intricate

DOI: 10.1021/acs.inorgchem.5b00048
Inorg. Chem. 2015, 54, 5204−5212

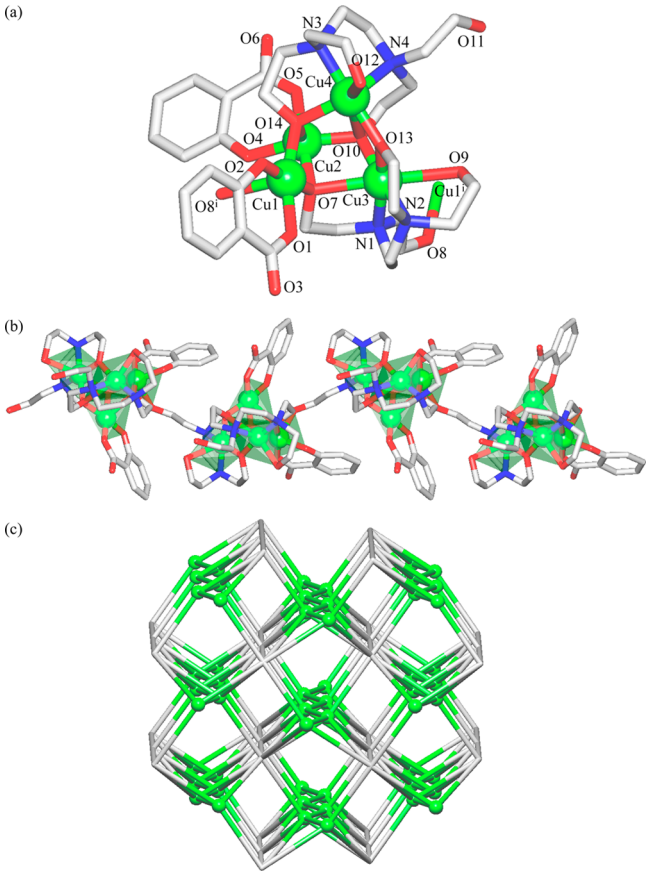

Figure 1. Structural fragments of **1** showing (a) a tetracopper(II) $[Cu_4(\mu_4\text{-}H_2edte)(\mu_5\text{-}H_2edte)(sal)_2]$ unit with an atom numbering scheme, (b) a 1D metal−organic chain with polyhedral representation of the coordination environments around Cu atoms, and (c) a topological representation of the underlying binodal 6,10-connected 3D supramolecular network. Further details: (a and b) H atoms omitted for clarity [Cu, green; O, red; N, blue; C, gray]; (c) view along the *a* axis, centroids of 6-connected $[Cu_4(H_2edte)_2(sal)_2]$ (green balls) and 10-connected $(H_2O)_{18}$ (gray) nodes. Selected distances (Å): Cu1−O1 1.927(6), Cu1−O2 1.890(6), Cu1−O7 1.956(5), Cu1−O8^i 2.432(6), Cu1−O14 1.970(6), Cu2−O4 1.902(6), Cu2−O5 1.908(7), Cu2−O7 1.975(6), Cu2−O10 1.921(5), Cu2−O14 2.404(6), Cu3−O7 2.395(5), Cu3−O9 2.648(8), Cu3−O10 1.943(6), Cu3−O13 1.941(6), Cu3−N1 2.099(6), Cu3−N2 1.990(8), Cu4−O10 2.900(6), Cu4−O12 2.428(8), Cu4−O13 1.901(6), Cu4−O14 1.988(6), Cu4−N3 2.009(8), Cu4−N4 2.071(7), Cu1···Cu2 3.129(2), Cu1···Cu3 3.624(1), Cu1···Cu4 3.453(1), Cu2···Cu3 3.156(2), Cu2···Cu4 3.387(2), Cu3···Cu4 3.322(2). Symmetry code: (i) $x + {}^1/_2, y, -z + {}^3/_2$.

infinite 1D $\{(H_2O)_{18}\}_n$ water tapes (Figure S3a in the SI), built from cyclic $(H_2O)_n$ (n = 8, 3) associates. Given the presence of some disorder, these water tapes can be roughly classified within the T8 general type according to the systematization introduced by Infantes and Motherwell.[21] These water tapes participate in multiple intermolecular hydrogen-bonding interactions with the host 1D metal−organic chains, thus extending the structure into a very complex 3D supramolecular network (Figure S4a in the SI). To gain further insight into this network, we have performed its topological analysis by following the concept of a simplified underlying net.[13] The structure of **1** underwent a significant simplification, namely involving the contraction of the $[Cu_4(H_2edte)_2(sal)_2]$ units and the $(H_2O)_{18}$ fragments of water tapes to the centroids that correspond to the 6- and 10-connected nodes, respectively. The

Scheme 2. Schematic Representation of (a) Regular, (b) Single-Open, and (c) Double-Open $[Cu_4O_4]$ Cubane Cores and (d) Their Simplified Topological Graph Showing a Uninodal 3-Connected Motif with 3M4-1 Topology and a Point Symbol of (3^3) and Ball-and-Stick Representation of Distorted (e) Single-Open $[Cu_4(\mu_2\text{-}O)(\mu_3\text{-}O)_3]$ and (f) Double-Open $[Cu_4(\mu_2\text{-}O)_2(\mu_3\text{-}O)_2]$ Cubane Cores in 1 and 2, Respectively[a]

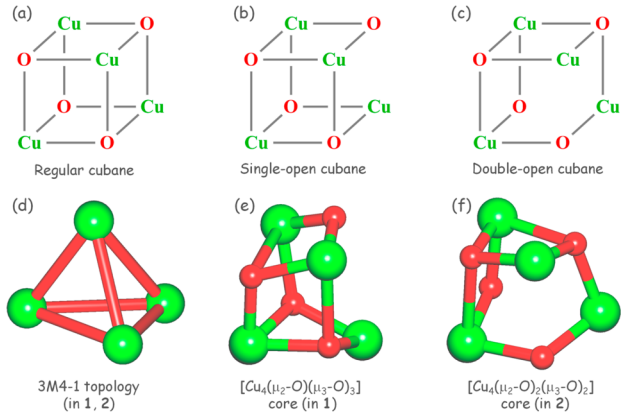

[a]Color code: Cu centers, green balls; O atoms, red balls.

resulting binodal 6,10-connected net (Figure 1c) has a point symbol of $(3^5.4^7.5^2.6)_2(3^8.4^{12}.5^{20}.6^4.7)$ and is topologically unique, as confirmed by a search of various databases.[1,13,22a]

The discrete 0D structure of **2** bears a neutral tetracopper(II) $[Cu_4(\mu_4\text{-}Hedte)_2(Hpmal)_2(H_2O)]$ unit (Figure 2a) and 7.5 crystallization water molecules. Although this Cu_4 unit resembles that of **1**, there are a few differences, which consist of (i) the compound's dimensionality (0D in **2** vs 1D in **1**), (ii) the presence of two monoprotonated μ_4-Hedte ligands in **2** versus μ_4- and μ_5-H_2edte in **1**, and (iii) the existence of three five-coordinate (Cu1, Cu3, and Cu4) and one six-coordinate (Cu2) Cu atoms in **2** versus a pair of five- and six-coordinate Cu centers in **1**. These differences lead to the formation of a slightly distinct double-open cubane $[Cu_4(\mu_2\text{-}O)_2(\mu_3\text{-}O)_2]$ core in **2** (Scheme 2c,f) with the Cu···Cu separations ranging from 3.102(1) to 3.548(2) Å (avg 3.309 Å). This core also has 3M4-1 topology (Scheme 2d). In **2**, the Cu1 and Cu4 centers show resembling distorted square-pyramidal $\{CuO_5\}$ environments (τ_5 = 0.16 and 0.12, respectively),[19a,b] which are filled by two O atoms of the chelating monoprotonated phenylmalonate(−) ligands [Cu1−O1 1.952(3) Å; Cu1−O3 1.937(3) Å; Cu4−O7 1.931(3) Å; Cu4−O8 1.923(3) Å] and the remaining O atoms coming from the Hedte moieties [Cu1−O4 1.966(3) Å; Cu1−O5 1.924(3) Å; Cu1−O12 2.303(3) Å; Cu4−O4 1.942(3) Å; Cu4−O12 1.946(3) Å] as well as a coordinated water molecule [only at the Cu4 center, Cu4−O7w 2.498(5) Å]. In contrast, the Cu3 atom features a $\{CuN_2O_3\}$ geometry that is better considered as a highly distorted trigonal-bipyramidal (τ_5 = 0.65 in **2**; τ_5 = 1 for idealized trigonal-bipyramidal geometry),[19a,b] which is filled by the equatorial N4, O6, and O12 atoms and the axial N3 and O11 atoms of Hedte moieties [Cu3−N4 2.021(4) Å; Cu3−O6 1.917(3) Å; Cu3−O12 2.012(3) Å; Cu3−N3 2.098(4) Å; Cu3−O11 2.292(3) Å]. The six-coordinate Cu2 atom exhibits a distorted octahedral $\{CuN_2O_4\}$ environment filled by the basal N1, N2, O5, and O6 atoms and the apical O4 and O14 atoms of Hedte ligands [Cu2−N1 2.088(4) Å; Cu2−N2 1.990(5) Å; Cu2−O5 1.932(3) Å; Cu2−O6 1.936(3) Å; Cu2−O4 2.439(3) Å;

DOI: 10.1021/acs.inorgchem.5b00048
Inorg. Chem. 2015, 54, 5204−5212

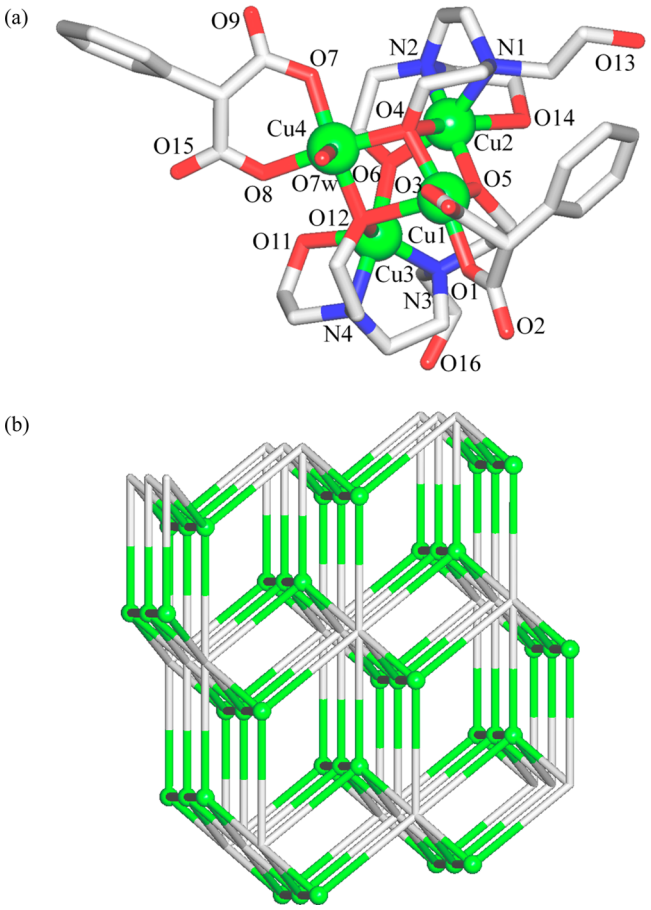

Figure 2. Structural fragments of **2** showing (a) a tetracopper(II) $[Cu_4(\mu_4\text{-Hedte})_2(Hpmal)_2(H_2O)]$ unit with atom numbering scheme and (b) a topological representation of the underlying binodal 6,8-connected 3D supramolecular network with 6,8T2 topology. Further details: (a) H atoms omitted for clarity [Cu, green; O, red; N, blue; C, gray]; (b) view along the *b* axis, centroids of 8-connected $[Cu_4(Hedte)_2(Hpmal)_2(H_2O)]$ (green balls) and 6-connected $(H_2O)_9$ (gray) nodes. Selected distances (Å): Cu1−O1 1.952(3), Cu1−O3 1.937(3), Cu1−O4 1.966(3), Cu1−O5 1.924(3), Cu1−O12 2.303(3), Cu2−N1 2.088(4), Cu2−N2 1.990(5), Cu2−O4 2.439(3), Cu2−O5 1.932(3), Cu2−O6 1.936(3), Cu2−O14 2.576(8), Cu3−N3 2.098(4), Cu3−N4 2.021(4), Cu3−O6 1.917(3), Cu3−O11 2.292(3), Cu3−O12 2.012(3), Cu4−O4 1.942(3), Cu4−O7 1.931(3), Cu4−O7w 2.498(5), Cu4−O8 1.923(3), Cu4−O12 1.946(3), Cu1···Cu2 3.159(1), Cu1···Cu3 3.423(1), Cu1···Cu4 3.102(1), Cu2···Cu3 3.352(1), Cu2···Cu4 3.548(2), Cu3···Cu4 3.269(1).

Cu2−O14 2.576(8) Å]. In **2**, most of the bonding parameters are comparable to those found in **1** and other Cu compounds derived from H_4edte.[5a,8] Because the reported Cu-edte derivatives are limited to a few mono- and dinuclear complexes,[5a,8] both compounds **1** and **2** not only represent the first examples of polynuclear copper clusters derived from H_4edte but also bear the first $[M_4O_4]$ cubane cores (Scheme 2) encountered in other transition-metal H_4edte-driven compounds.[1] Hence, the present work opens up the application of H_4edte toward the design of copper clusters.

Furthermore, several crystallization water molecules in **2** are assembled into discrete $(H_2O)_9$ clusters that comprise a linear $(H_2O)_7$ motif with two branched water groups (Figure S3b in the SI). These clusters can be classified within the D7 type.[21] An intense pattern of intermolecular hydrogen-bonding interactions involving such water clusters, discrete water (O4w and O6w) molecules, and tetracopper(II) units leads to the generation of an intricate 3D supramolecular network (Figure S4b in the SI). For topological analysis,[13] this network has been simplified by reducing the 8-connected $[Cu_4(Hedte)_2(Hpmal)_2(H_2O)]$ and 6-connected $(H_2O)_9$ moieties to their centroids and eliminating discrete water molecules. The resulting binodal 6,8-connected net (Figure 2b) features 6,8T2 topology[13,22] with a point symbol of $(3^2.4^{12}.5^{10}.6^4)(3^2.4^6.5^6.6)_2$. This topological type is rare and was only identified in one compound.[22b]

Magnetic Studies. The magnetic properties of **1** and **2** were investigated over the temperature range of 1.8−300 K. Plots of the magnetic susceptibility χ_m and $\chi_m T$ product versus T (χ_m is the molar magnetic susceptibility for four Cu^{II} ions) are given in Figures S5 in the SI and 3a, respectively. At room

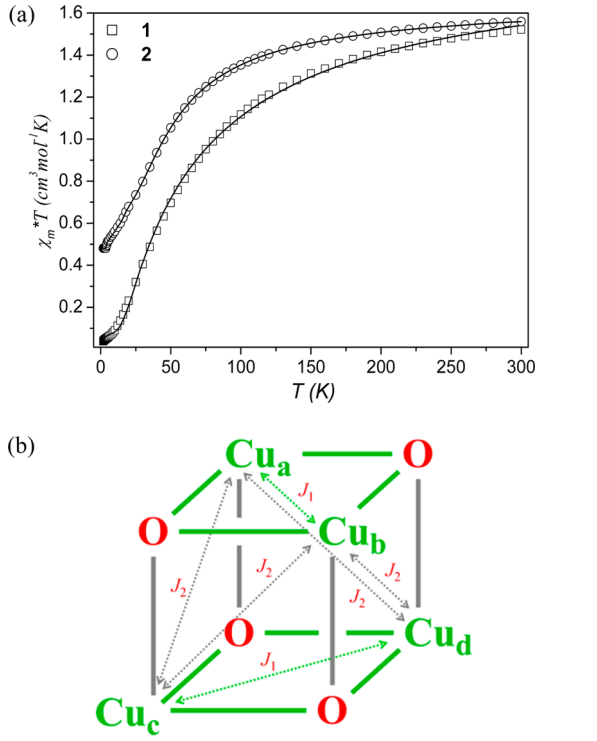

Figure 3. (a) Temperature dependence of experimental $\chi_m T$ (χ_m per 4 Cu^{II} atoms) for **1** and **2**. The solid lines (for **1** and **2**) are the calculated curves derived from eq 1. (b) Schematic representation of the exchange coupling pattern in the model 2 + 4 $[Cu_4O_4]$ cubane core.

temperature, $\chi_m T$ is 1.52 and 1.59 cm^3 K mol^{-1} for **1** and **2**, respectively; these values are consistent with the presence of four uncoupled Cu^{II} ions $[\chi_m T = 4(N\beta^2 g^2/3k)S(S+1) = 1.5]$ cm^3 K mol^{-1}, assuming $g = 2.1$ and $S = {}^1/_2$, where N, β, g, k, S, and T have their usual meaning].[23] Upon cooling, $\chi_m T$ continuously decreases, reaching almost zero at 1.8 K in **1**. These features are characteristic of an overall antiferromagnetic coupling in **1**, which leads to a low-lying spin state ($S = 0$). Additionally, the maximum of the magnetic susceptibility is observed in the χ_m versus T plot for **1** at 45 K (Figure S5 in the SI). The increase of χ_m at low temperature indicates the presence of a small amount of paramagnetic impurities ($S = {}^1/_2$). The absence of a maximum in the χ_m curve of **2** may indicate that the possible coupling is weaker in this compound.

DOI: 10.1021/acs.inorgchem.5b00048
Inorg. Chem. 2015, 54, 5204−5212

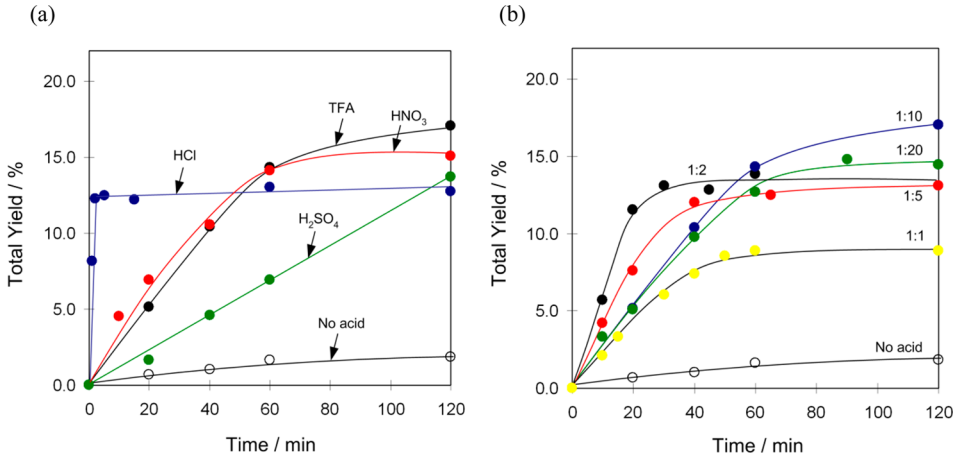

Figure 4. Oxidation of cyclohexane to cyclohexanol and cyclohexanone by H_2O_2 in the presence of precatalyst **1**. (a) Evolution of the total product yield with time in the absence and in the presence of different acid promoters (TFA, HNO_3, H_2SO_4, or HCl; 0.1 mmol). (b) Effect of the TFA amount on the evolution of the total product yield with time (**1**/TFA molar ratios: 1:0, 1:1, 1:2, 1:5, 1:10, and 1:20). General conditions: C_6H_{12} (2 mmol), H_2O_2 (50% aqueous, 10 mmol), **1** (0.01 mmol), TFA (0–0.2 mmol), 50 °C, MeCN (up to 5 mL). For similar data with precatalyst **2**, see Figure S8 in the SI.

To confirm the nature of the ground state of **1** and **2**, we have investigated variation of the magnetization (M) with respect to the field (H) at 2 K. The results are shown in Figure S6 in the SI, where the molar magnetization M (per Cu_4 entity) is expressed in μ_B units. The magnetization curves for **1** and **2** were reproduced by the equation $M = g\beta SNB_s(x)$ ($S = 4S_{Cu}$), where $B_s(x)$ is the Brillouin function and $x = g\beta H/kT$.[23] The experimental values for **1** and **2** are much lower than those calculated using the Brillouin function for four noninteracting Cu^{II} ions. This feature agrees with the global antiferromagnetic coupling within the four Cu^{II} ions in **1** and **2**.

In compounds **1** and **2**, four Cu^{II} ions (Cu_a, Cu_b, Cu_c, and Cu_d) occupy alternating cubane vertices and have six Cu···Cu exchange interactions. Considering the presence of two short (3.102–3.159 Å) and four rather long (3.269–3.624 Å) Cu···Cu separations in **1** and **2**, their $[Cu_4O_4]$ cubane cores can be classified within the 2 + 4 type[24] and analyzed using the spin Hamiltonian given in eq 1:[23]

$$H = -J_1(\hat{S}_a\hat{S}_b + \hat{S}_c\hat{S}_d) - J_2(\hat{S}_a\hat{S}_c + \hat{S}_a\hat{S}_d + \hat{S}_b\hat{S}_c + \hat{S}_b\hat{S}_d) \quad (1)$$

where J_1 and J_2 are the intra- and interdinuclear exchange coupling constants between the local spins within the $[Cu_4O_4]$ cubane core (Figure 3b). The molar magnetic susceptibility for **1** and **2** is given in the SI. A least-squares fitting of the experimental data leads to the following values: $J_1 = -53.3(3)$ cm^{-1}, $J_2 = -23.7(5)$ cm^{-1}, $g = 2.09(1)$, and $\rho = 5.4\%$ ($R = 2.5 \times 10^{-4}$) for **1** and $J_1 = -48.3(4)$ cm^{-1}, $J_2 = -1.2(1)$ cm^{-1}, $g = 2.24(2)$, and $\rho = 3.4\%$ ($R = 2.2 \times 10^{-4}$) for **2**. The criterion applied to determine the best fit was based on the minimization of the sum of squares of the deviation, $R = \sum(\chi_{exp}T - \chi_{calc}T)^2/\sum(\chi_{exp}T)^2$. The calculated curves for **1** and **2** (solid lines in Figure 3a) match very well with the experimental magnetic data in the whole temperature range. The obtained values of J_1 and J_2 indicate an antiferromagnetic coupling between the Cu^{II} ions within the tetracopper(II) clusters in **1** and **2**.

Magnetostructural correlations for the hydroxo- and alkoxo-bridged copper(II) compounds were proposed by Hatfield and co-workers.[25] They found that the nature and strength of the magnetic exchange coupling are mainly affected by the Cu···Cu distance and the Cu–O–Cu bridging angle (α). In general, the antiferromagnetic coupling is observed for large Cu–O–Cu bond angles and long Cu···Cu separations, whereas the ferromagnetic interaction is favored for small Cu–O–Cu bond angles (<97.5°), which usually imply shorter Cu···Cu distances. Although the Cu–O–Cu angles and Cu···Cu distances are the most crucial geometrical parameters, the coupling constants can also be modulated by other structural features. The values of J_1 obtained for **1** and **2** are roughly in agreement with the earlier reported figures for this parameter in alkoxo-bridged $[Cu_4O_4]$ cubanes.[24,26–28] The presence of antiferromagnetic interactions in **1** and **2** is certainly attributed to the relatively large Cu–O–Cu angles (mean value above 100°) and rather long Cu···Cu separations (avg 3.329 or 3.309 Å for **1** or **2**, respectively). However, the calculated J_2 parameters for **1** and **2** have negative values in contrast to the weakly ferromagnetic interactions generally found in the literature.[27] It was proposed that these interactions are practically independent of the geometrical parameters.[24c] In general, the magnetic behavior of **1** and **2** is in agreement with the majority of alkoxo-bridged tetranuclear copper(II) compounds. Although **1** and **2** show rather similar magnetic features, some distinction in their behavior may be caused by the 1D chain structure of **1** and the different coordination geometries of Cu atoms in these compounds.

Mild Catalytic Oxidation of Alkanes. Following our interest in the oxidative functionalization of alkanes under mild conditions catalyzed by multicopper(II) complexes,[3,5b–e,29] we probed both compounds **1** and **2** as precatalysts for the oxidation by H_2O_2 of various cyclic and linear C_5–C_8 alkanes to the corresponding alcohols and ketones. The oxidation reactions were carried out in an aqueous MeCN medium at 50 °C and in the presence of an acid promoter (Table 2). Cyclohexane was studied in detail as a recognized model substrate[30] (Figures 4 and S8–S10 in the SI), whereas other alkanes were oxidized under optimized conditions.

In the oxidation of cyclohexane to cyclohexanol and cyclohexanone, both compounds **1** and **2** exhibit rather low activity (2–4% total yields) unless a small amount of acid promoter is added (Figures 4 and S9 in the SI), leading to a pronounced yield growth. To examine whether the type of acid promoter affects the efficiency of cyclohexane oxidation,[3,31] we

DOI: 10.1021/acs.inorgchem.5b00048
Inorg. Chem. 2015, 54, 5204–5212

tested the activity of precatalysts **1** (Figure 4a) and **2** (Figure S9a in the SI) in the presence of various acid promoters, namely, trifluoroacetic (TFA), nitric (HNO_3), sulfuric (H_2SO_4), and hydrochloric (HCl) acids. Compounds **1** and **2** show rather similar behavior. Although the type of promoter affects significantly the reaction rate of cyclohexane oxidation, the final product yields are comparable when using different acids. In the C_6H_{12} oxidation, the **1**/TFA and **2**/TFA systems result in total yields of 17 and 18% after 120 min, respectively. The kinetic curves of product accumulation in the **1**/HNO_3 and **2**/HNO_3 systems are very close to those in the presence of TFA promoter, leading to ∼15% yields. Although the oxidation of cyclohexane is slower when using H_2SO_4 as a promoter, total yields of 14 and 18% are achieved with precatalysts **1** and **2**, respectively. Interestingly, the oxidation of C_6H_{12} is extremely fast in the presence of HCl and the reaction is completed in 3 min but results in inferior product yields (13%) in both systems containing **1** or **2**. According to the literature background,[3,29,31] the role of an acid promoter consists of its participation in proton-transfer steps, activation of the precatalyst by protonation of ligands and unsaturation of the metal centers, and augmentation of the oxidative properties of H_2O_2 and prevention of its decomposition (i.e., catalase activity).

Given the good promoting behavior of TFA, the effect of its amount was investigated in the cyclohexane oxidation with precatalysts **1** (Figure 4b) and **2** (Figure S9b in the SI). A very small amount of TFA (1−2 equiv relative to the precatalyst) is enough to promote the activity of both tetracopper(II) compounds and increase the reaction rate of C_6H_{12} oxidation (Figure S10 in the SI). In the case of **1**, the maximum value of the initial reaction rate (W_0) was achieved at a **1**/TFA molar ratio of 1:2, corresponding to a total product yield of 14%. A further increase of the TFA amount up to 10 and 20 equiv results in a decrease of W_0 (Figure S10a in the SI), without significantly affecting the efficiency of the precatalyst and leading to comparable total product yields of 17 and 15%, respectively (Figure 4b). In the cyclohexane oxidation by the **2**/TFA/H_2O_2 system, the maximum initial rate W_0 is attained at a **2**/TFA molar ratio of 1:5 (Figure S10b in the SI), corresponding to a total product yield of 10%. A further increase of the TFA loading has almost no effect on W_0 but gives a higher product yield (18% at a **2**/TFA molar ratio of 1:10; Figure S9b in the SI).

It should be mentioned that precatalysts **1** and **2** are not intact during the catalytic experiments and in the presence of an acid promoter and H_2O_2 lead to the formation of homogeneous catalytically active species, eventually via the additional protonation and partial decoordination of amino alcohol or aromatic carboxylate ligands.[3,16,29,31] Although a detailed investigation of catalytic intermediates was out of the main scope of the current work, we performed an electrospray ionization mass spectrometry (ESI-MS) study of precatalyst **1** in a MeCN/H_2O medium before and after its treatment with TFA promoter and H_2O_2 oxidant, using conditions equal to those of the catalytic tests. The most characteristic peaks observed in the ESI-MS(−) spectrum of **1** are due to the tetracopper $[Cu_4(H_2edte)_2(sal)_2 - H]^-$ (m/z 994) and $[Cu_4(H_2edte)_2(sal)_2 - CH_2CH_2OH]^-$ (m/z 949) fragments, with the latter corresponding to an ESI-induced cleavage of one hydroxyethyl group in H_2edte. The ESI-MS(+) plot of **1** also reveals tetracopper fragments, namely, $[Cu_4(Hedte)_2(Hsal)]^+$ (m/z 858) and $[Cu_4(Hedte)(sal)(H_2O) - CH_2CH_2OH]^+$ (m/z 597), corresponding to fragmentations with the elimination of one carboxylate or one carboxylate along with one amino alcohol ligand. After the treatment of **1** with TFA and H_2O_2, the obtained ESI-MS(±) patterns still display all of the above-mentioned fragments, although their intensity has decreased with the exception of $[Cu_4(Hedte)(sal)(H_2O) - CH_2CH_2OH]^+$ (m/z 597), which continues to be the most intense peak in a positive mode. In addition, new $[Cu_4(edte)(sal)(H_2O)_2(MeCN)]^-$ (m/z 699) and $[Cu_4(Hedte)_2(H_2O) - CH_2CH_2OH]^-$ (m/z 649) fragments have emerged in the ESI-MS(−) spectrum. These data suggest that various tetracopper species derived from the parent precatalyst **1** upon decoordination of one H_2edte and one sal ligands or a pair of salicylate moieties can potentially constitute the catalytically active species.

The **1**/TFA/H_2O_2 and **2**/TFA/H_2O_2 systems can also be applied for the oxidation of other alkanes, including various cyclic and linear C_5−C_8 hydrocarbons (Table 2). Among cyclic alkanes, the oxidation of cycloheptane appears to be the most efficient, resulting in up to 20−21% total yields of cycloheptanol and cycloheptanone. Cyclooctane and cyclohexane are slightly less reactive substrates (14−19% total product yields), followed by cyclopentane, which is the least active cycloalkane (7−9% total product yield). In contrast to cycloalkanes, linear C_5−C_8 alkanes are less reactive, showing the maximum total yields of oxidation products (isomeric alcohols and ketones) of 9−10% in the case of *n*-heptane, followed by *n*-hexane (4−6%), *n*-octane (4−5%), and *n*-pentane (3%).

By analogy with other multicopper(II) precatalysts for alkane oxidation by H_2O_2, the determined regioselectivity, bond-selectivity, and stereoselectivity parameters (see Table S2 and additional discussion in the SI) are comparable to those previously reported[3,29] for copper-based catalytic systems operating with hydroxyl radicals, thus suggesting their involvement as principal oxidizing species. Considering the related literature background,[3,29,31] it is possible to assume the following mechanistic steps for alkane oxidation. Thus, an acid promoter interacts with a copper precatalyst, causing the formation of labile sites (via an additional protonation and partial decoordination of amino alcohol and/or carboxylate ligands) and the generation of active copper(II) species. These participate in the formation of $HO^\bullet$ radicals from H_2O_2,[3,29c] which then abstract H atoms from an alkane, generating the alkyl radicals ($R^\bullet$). These react further with O_2 (e.g., from air), giving rise to the $ROO^\bullet$ radicals, which are transformed to alkyl hydroperoxides (ROOH) as primary intermediate products. Alkyl hydroperoxides rapidly decompose to furnish the corresponding alcohols and ketones as final products.[3,29,31,32]

CONCLUSIONS

The current study has widened a still very limited application of H_4edte as an aqua-soluble, commercially available, and versatile multidentate building block for the design of new multicopper compounds, namely resulting in the aqueous medium self-assembly generation of two tetracopper(II) products, **1** and **2**. The type of ancillary aromatic carboxylate ligand plays an important structure-driven role in defining the dimensionality and kind of the tetracopper(II) cubane core in the obtained compounds. Apart from representing the first polynuclear copper clusters derived from H_4edte, both **1** and **2** also reveal the first examples of transition-metal $[M_4O_4]$ cubane cores driven by this amino alcohol.[1]

Another structural feature concerns the fact that the metal−organic chains in **1** or discrete clusters in **2** also act as matrixes

DOI: 10.1021/acs.inorgchem.5b00048
Inorg. Chem. 2015, 54, 5204−5212

to host numerous crystallization water molecules, which are assembled into the intricate $\{(H_2O)_{18}\}_n$ water tapes or discrete $(H_2O)_9$ clusters, respectively. These water aggregates play a key role in sewing the metal−organic hosts into very complex 3D supramolecular frameworks. Their topological analysis has disclosed either binodal 6,10- or 6,8-connected underlying 3D nets with the hitherto undocumented or rare topologies in **1** or **2**, respectively. Thus, the present work not only widens the growing family of water assemblies detected in coordination compounds[35,36] but also contributes toward the identification of novel topological networks, which is currently a sweeping research direction in crystal engineering.[13,22]

The magnetic properties of the obtained compounds were investigated, indicating a predominant antiferromagnetic coupling between Cu^{II} centers within the $[Cu_4O_4]$ cores. Although these cores in **1** and **2** reveal a number of structural differences, both compounds show essentially similar magnetic behavior, which is also in good agreement with other alkoxo-bridged tetranuclear copper(II) derivatives.

Besides, the present work showed that the obtained copper(II) derivatives can act as bioinspired oxidation precatalysts[33] with some relevance to particulate methane monooxygenase (a unique copper enzyme that contains an active site based on a multicopper cluster with an N,O environment capable of hydroxylating alkanes).[34] In fact, both compounds **1** and **2** are precatalysts in the mild oxidation, by aqueous H_2O_2 in acidic MeCN/H_2O media, of different cyclic and linear C_5−C_8 alkanes to produce the corresponding alcohols and ketones. Because these reactions also require the presence of an acid cocatalyst, the promoting influence of different acids (TFA, HNO_3, H_2SO_4, and HCl) was studied, revealing the highest activity in the systems containing TFA. The substrate versatility and different selectivity parameters were also investigated.

Further research will be pursued toward the exploration of H_4edte and related amino alcohol building blocks in the design of novel multicopper(II) cores, their incorporation into metal−organic frameworks, and the study of the magnetic and catalytic properties of the obtained materials. These and other research directions are currently in progress.

■ ASSOCIATED CONTENT

Supporting Information

Materials and methods, additional discussion of IR and EPR spectra, thermogravimetric analyses, magnetic and catalytic studies, as well as thermogravimetric−differential thermal analysis plots (Figures S1 and S2), structural representations of water clusters (Figure S3), 3D supramolecular networks (Figure S4), molar magnetic susceptibility plots (Figure S5), field dependence of the magnetization (Figure S6), EPR spectra (Figure S7), additional catalytic results (Table S1 and Figures S8−S10), selectivity parameters (Table S2), and crystallographic files for **1** and **2** in CIF format (CCDC 1042427−1042428). The Supporting Information is available free of charge on the ACS Publications website at DOI: 10.1021/acs.inorgchem.5b00048.

■ AUTHOR INFORMATION

Corresponding Author

*E-mail: kirillov@ist.utl.pt.

Notes

The authors declare no competing financial interest.

■ ACKNOWLEDGMENTS

This work was supported by the Foundation for Science and Technology (Projects PTDC/QUI-QUI/121526/2010, IF/01395/2013/CP1163/CT005, RECI/QEQ-QIN/0189/2012, PEst-OE/QUI/UI0100/2013, SFRH/BPD/78854/2011, and REM 2013), Portugal. We thank Dr. M. C. Oliveira and A. Dias for ESI-MS(±) measurements.

■ REFERENCES

(1) See the Cambridge Structural Database (CSD, version 5.36, 2015): Allen, F. H. *Acta Crystallogr.* **2002**, *B58*, 380−388.

(2) For reviews, see: (a) Singh, A.; Mehrotra, R. C. *Coord. Chem. Rev.* **2004**, *248*, 101−118. (b) Verkade, J. G. *Acc. Chem. Res.* **1993**, *26*, 483−489.

(3) Kirillov, A. M.; Kirillova, M. V.; Pombeiro, A. J. L. *Coord. Chem. Rev.* **2012**, *256*, 2741−2759.

(4) For selected recent examples, see: (a) Sanz, S.; Frost, J. M.; Pitak, M. B.; Coles, S. J.; Piligkos, S.; Lusby, P. J.; Brechin, E. K. *Chem. Commun.* **2014**, *50*, 3310−3312. (b) Gao, Q.; Li, F.-G.; Wang, Y.-C.; Xu, L.; Bai, J.; Wang, Y. *Dalton Trans.* **2014**, *43*, 941−944. (c) Abbas, G.; Lan, Y.; Mereacre, V.; Buth, G.; Sougrati, M. T.; Grandjean, F.; Long, G. J.; Anson, C. E.; Powell, A. K. *Inorg. Chem.* **2013**, *52*, 11767−11777. (d) Baniodeh, A.; Mereacre, V.; Magnani, N.; Lan, Y.; Wolny, J. A.; Schunemann, V.; Anson, C. E.; Powell, A. K. *Chem. Commun.* **2013**, *49*, 9666−9668. (e) Hosseinian, S. R.; Tangoulis, V.; Menelaou, M.; Raptopoulou, C. P.; Psycharis, V.; Dendrinou-Samara, C. *Dalton Trans.* **2013**, *42*, 5355−5366. (f) Xu, G.; Lv, J.; Guo, P.; Zhou, Z.; Du, Z.; Xie, Y. *CrystEngComm* **2013**, *15*, 4473−4482.

(5) (a) Dias, S. S. P.; André, V.; Kłak, J.; Duarte, M. T.; Kirillov, A. M. *Cryst. Growth Des.* **2014**, *14*, 3398−3407. (b) Kirillova, M. V.; Kirillov, A. M.; Martins, A. N. C.; Graiff, C.; Tiripicchio, A.; Pombeiro, A. J. L. *Inorg. Chem.* **2012**, *51*, 5224−5234. (c) Kirillov, A. M.; Karabach, Y. Y.; Kirillova, M. V.; Haukka, M.; Pombeiro, A. J. L. *Cryst. Growth Des.* **2012**, *12*, 1069−1074. (d) Karabach, Y. Y.; da Silva, M. F. C. G.; Kopylovich, M. N.; Gil-Hernández, B.; Sanchiz, J.; Kirillov, A. M.; Pombeiro, A. J. L. *Inorg. Chem.* **2010**, *49*, 11096−11105. (e) Kirillov, A. M.; Coelho, J. A. S.; Kirillova, M. V.; da Silva, M. F. C. G.; Nesterov, D. S.; Gruenwald, K. R.; Haukka, M.; Pombeiro, A. J. L. *Inorg. Chem.* **2010**, *49*, 6390−6392.

(6) (a) Zhou, A.-J.; Leng, J.-D.; Hu, J.-S.; Tong, M.-L. *Dalton Trans.* **2013**, *42*, 9428−9431. (b) Saha, A.; Abboud, K. A.; Christou, G. *Inorg. Chem.* **2011**, *50*, 12774−12784. (c) Saha, A.; Thompson, M.; Abboud, K. A.; Wernsdorfer, W.; Christou, G. *Inorg. Chem.* **2011**, *50*, 10476−10485. (d) Bagai, R.; Abboud, K. A.; Christou, G. *Inorg. Chem.* **2008**, *47*, 621−631. (e) Zhou, A.-J.; Qin, L.-J.; Beedle, C. C.; Ding, S.; Nakano, M.; Leng, J.-D.; Tong, M.-L.; Hendrickson, D. N. *Inorg. Chem.* **2007**, *46*, 8111−8113.

(7) (a) Graham, K.; Douglas, F. J.; Mathieson, J. S.; Moggach, S. A.; Schnack, J.; Murrie, M. *Dalton Trans.* **2011**, *40*, 12271−12276. (b) Akhtar, M. N.; Mereacre, V.; Novitchi, G.; Tuchagues, J.-P.; Anson, C. E.; Powell, A. K. *Chem.—Eur. J.* **2009**, *15*, 7278−7282. (c) Zhou, A.-J.; Liu, J.-L.; Herchel, R.; Leng, J.-D.; Tong, M.-L. *Dalton Trans.* **2009**, 3182−3192. (d) Bagai, R.; Daniels, M. R.; Abboud, K. A.; Christou, G. *Inorg. Chem.* **2008**, *47*, 3318−3127.

(8) (a) Kumar, R.; Obrai, S.; Kaur, A.; Hundal, G.; Meehnian, H.; Jana, A. K. *Polyhedron* **2013**, *56*, 55−61. (b) de Sousa, A. S.; Fernandes, M. A. *Polyhedron* **2013**, *21*, 1883−1888. (c) Kirillov, A. M.; Kirillova, M. V.; Shul'pina, L. S.; Figiel, P. J.; Gruenwald, K. R.; da Silva, M. F. C. G.; Haukka, M.; Pombeiro, A. J. L.; Shul'pin, G. B. *J. Mol. Catal. A: Chem.* **2011**, *350*, 26−34.

(9) *APEX2*; Bruker Analytical Systems: Madison, WI, 2005.

(10) Altomare, A.; Burla, M. C.; Camalli, M.; Cascarano, G. L.; Giacovazzo, C.; Guagliardi, A.; Moliterni, A. G. G.; Polidori, G.; Spagna, R. *J. Appl. Crystallogr.* **1999**, *32*, 115−119.

(11) Sheldrick, G. M. *Acta Crystallogr.* **2008**, *A64*, 112−122.

(12) Farrugia, L. J. *J. Appl. Crystallogr.* **1999**, *32*, 837−838.

(13) (a) Blatov, V. A.; Shevchenko, A. P.; Proserpio, D. M. *Cryst. Growth Des.* **2014**, *14*, 3576−3586. (b) Blatov, V. A. *IUCr CompComm*

DOI: 10.1021/acs.inorgchem.5b00048
Inorg. Chem. 2015, 54, 5204−5212

Newsletter **2006**, *7*, 4−38. (c) Zolotarev, P. N.; Arshad, M. N.; Asiri, A. M.; Al-amshany, Z. M.; Blatov, V. A. *Cryst. Growth Des.* **2014**, *14*, 1938−1949. (d) Baburin, I. A.; Blatov, V. A.; Carlucci, L.; Ciani, G.; Proserpio, D. M. *Cryst. Growth Des.* **2008**, *8*, 519−539.
(14) Spek, A. L. *Acta Crystallogr.* **2009**, *D65*, 148−155.
(15) Bain, G. A.; Berry, J. F. *J. Chem. Educ.* **2008**, *85*, 532−536.
(16) (a) Shul'pin, G. B. *J. Mol. Catal. A: Chem.* **2002**, *189*, 39−66. (b) Shul'pin, G. B. *C. R. Chim.* **2003**, *6*, 163−178. (c) Shul'pin, G. B. *Mini-Rev. Org. Chem.* **2009**, *6*, 95−104.
(17) (a) Camaioni, D. M.; Lilga, M. A.; Bays, J. T.; Linehan, J. C.; Shaw, W. J.; Birnbaum, J. C. *Abstr. Pap. Am. Chem. Soc.* **1999**, *218*, U619−U620. (b) Camaioni, D. M.; Bays, J. T.; Shaw, W. J.; Linehan, J. C.; Birnbaum, J. C. *J. Org. Chem.* **2001**, *66*, 789−795.
(18) (a) Pasan, J.; Sanchiz, J.; Ruiz-Perez, C.; Lloret, F.; Julve, M. *Inorg. Chem.* **2005**, *44*, 7794−7801. (b) Pasan, J.; Sanchiz, J.; Ruiz-Perez, C.; Campo, J.; Lloret, F.; Julve, M. *Chem. Commun.* **2006**, 2857−2859.
(19) (a) Yang, L.; Powell, D. R.; Houser, R. P. *Dalton Trans.* **2007**, 955−964. (b) Addison, A. W.; Rao, T. N.; Reedijk, J.; van Rijn, J.; Verschoor, G. C. *J. Chem. Soc., Dalton Trans.* **1984**, 1349−1356. (c) Bondi, A. *J. Phys. Chem.* **1964**, *68*, 441−451.
(20) (a) Kostakis, G. E.; Blatov, V. A.; Proserpio, D. M. *Dalton Trans.* **2012**, *41*, 4634−4640. (b) Kostakis, G. E.; Perlepes, S. P.; Blatov, V. A.; Proserpio, D. M.; Powell, A. K. *Coord. Chem. Rev.* **2012**, *256*, 1246−1278.
(21) Infantes, L.; Motherwell, S. *CrystEngComm* **2002**, *4*, 454−461.
(22) (a) The Reticular Chemistry Structure Resource Database: O'Keeffe, M.; Peskov, M. A.; Ramsden, S. J.; Yaghi, O. M. *Acc. Chem. Res.* **2008**, *30*, 1782−1789. (b) He, X.; Lu, C.-Z.; Wu, C.-D.; Chen, L.-J. *Eur. J. Inorg. Chem.* **2006**, 2491−2503.
(23) Kahn, O. *Molecular Magnetism*; VCH: New York, 1993.
(24) (a) Ruiz, E.; Rodríguez-Fortea, A.; Alemany, P.; Alvarez, S.; Cano, J. *J. Am. Chem. Soc.* **1997**, *119*, 1297−1303. (b) Ruiz, E.; Rodríguez-Fortea, A.; Alemany, P.; Alvarez, S. *Polyhedron* **2001**, *20*, 1323−1327. (c) Tercero, J.; Ruiz, E.; Alvarez, S.; Rodriguez-Fortea, A.; Alemany, P. *J. Mater. Chem.* **2006**, *16*, 2729−2735.
(25) Crawford, V. H.; Richardson, H. W.; Wasson, J. R.; Hodgson, D. J.; Hatfield, W. E. *Inorg. Chem.* **1976**, *15*, 2107−2110.
(26) (a) Sletten, J.; Sorensen, A.; Julve, M.; Journaux, Y. *Inorg. Chem.* **1990**, *29*, 5054−5058. (b) Eberhardt, J. K.; Glaser, T.; Hoffmann, R. D.; Fröhlich, R.; Würsthwein, E. U. *Eur. J. Inorg. Chem.* **2005**, 1175−1181. (c) Tan, X. S.; Fujii, Y.; Nukada, R.; Mikuriya, M.; Nakano, Y. *J. Chem. Soc., Dalton Trans.* **1999**, 2415−2416.
(27) (a) Fallon, G. D.; Moubaraki, B.; Murray, K. S.; Van der Bergen, A. M.; West, B. O. *Polyhedron* **1993**, *12*, 1989−2000. (b) Wang, S.; Zheng, J.-C.; Hall, J. R.; Thompson, L. K. *Polyhedron* **1994**, *13*, 1039−1044. (c) Xie, Y.; Bu, W.; Xu, X.; Jiang, H.; Liu, Q.; Xue, Y.; Fan, Y. *Inorg. Chem. Commun.* **2001**, *4*, 558−560. (d) Burkhardt, A.; Spielberg, E. T.; Görls, H.; Plass, W. *Inorg. Chem.* **2008**, *47*, 2485−2493.
(28) Marino, N.; Armentano, D.; Mastropietro, T. F.; Julve, M.; De Munno, G.; Martínez-Lillo, J. *Inorg. Chem.* **2013**, *52*, 11934−11943.
(29) (a) Kirillov, A. M.; Kirillova, M. V.; Pombeiro, A. J. L. *Adv. Inorg. Chem.* **2013**, *65*, 1−31. (b) Kirillova, M. V.; Kirillov, A. M.; Mandelli, D.; Carvalho, W. A.; Pombeiro, A. J. L.; Shul'pin, G. B. *J. Catal.* **2010**, *272*, 9−17. (c) Kirillova, M. V.; Kozlov, Y. N.; Shul'pina, L. S.; Lyakin, O. Y.; Kirillov, A. M.; Talsi, E. P.; Pombeiro, A. J. L.; Shul'pin, G. B. *J. Catal.* **2009**, *268*, 26−38.
(30) Schuchardt, U.; Cardoso, D.; Sercheli, R.; Pereira, R.; da Cruz, R. S.; Guerreiro, M. C.; Mandelli, D.; Spinace, E. V.; Pires, E. L. *Appl. Catal., A* **2001**, *211*, 1−17.
(31) Kirillov, A. M.; Shul'pin, G. B. *Coord. Chem. Rev.* **2013**, *257*, 732−754.
(32) (a) Shul'pin, G. B. *Dalton Trans.* **2013**, *42*, 12794−12818. (b) Shul'pin, G. B. *Org. Biomol. Chem.* **2010**, *8*, 4217−4228.
(33) (a) Kirillov, A. M. *Coord. Chem. Rev.* **2011**, *255*, 1603−1622. (b) Kirillova, M. V.; Kirillov, A. M.; da Silva, M. F. C. G.; Kopylovich, M. N.; Fraústo da Silva, J. J. R.; Pombeiro, A. J. L. *Inorg. Chim. Acta* **2008**, *361*, 1728−1737. (c) Fernandes, R. R.; Kirillov, A. M.; da Silva, M. F. C. G.; Ma, Z.; da Silva, J. A. L.; Fraústo da Silva, J. J. R.; Pombeiro, A. J. L. *Cryst. Growth Des.* **2008**, *8*, 782−785.
(34) Nangia, A. Water Clusters in Crystal Hydrates. In *Encyclopedia of Supramolecular Chemistry - Update*; Atwood, J. L., Steed, J. W., Eds.; Taylor & Francis: London, 2007; Vol. *1.1*, pp 1−9.
(35) (a) Brissos, R. S.; Garcia, S.; Presa, A.; Gamez, P. *Comments Inorg. Chem.* **2011**, *32*, 219−245. (b) Gamez, P.; Aubel, P. G.; Driessen, W. L.; Reedijk, J. *Chem. Soc. Rev.* **2001**, *30*, 376−385.
(36) (a) Himes, R. A.; Karlin, K. D. *Curr. Opin. Chem. Biol.* **2009**, *13*, 119−131. (b) Lieberman, R. L.; Rosenzweig, A. C. *Nature* **2005**, *434*, 177−182.

DOI: 10.1021/acs.inorgchem.5b00048
Inorg. Chem. 2015, 54, 5204−5212